Available online at www.sciencedirect.com

SciVerse ScienceDirect

Ceramics International 39 (2013) 701–708

CERAMICS INTERNATIONAL

www.elsevier.com/locate/ceramint

Synthesis and luminescence properties of broad band greenish-yellow emitting $LnVO_4:Bi^{3+}$ and $(Ln1, Ln2)VO_4:Bi^{3+}$ (Ln = La, Gd and Y) as down conversion phosphors

U. Rambabu, Sang-Do Han*

Korea Institute of Energy Research (KIER), Daejeon 305-343, Republic of Korea

Received 6 June 2012; received in revised form 23 June 2012; accepted 25 June 2012
Available online 1 July 2012

Abstract

$Ln_{0.97}VO_4:Bi^{3+}_{0.03}$ and $(Ln1_{0.5}, Ln2_{0.5})_{0.97}VO_4:Bi^{3+}_{0.03}$ (where Ln = La, Gd and Y) down conversion (DC) phosphors have been synthesized by a novel co-precipitation technique followed by heat-treatment. The influence of lanthanide host composition on crystal structure, luminescence and pertinent optical properties have been investigated by various spectroscopic techniques: XRD, SEM, FT-IR and PL. The produced phosphors have exhibited an intense greenish-yellow emission, upon UV-irradiation. A broad band excitation (280–350 nm) ascribed to $^1S_0 \rightarrow {}^3P_1$ and an intense broad greenish-yellow emission band (400–700 nm) attributed to $^3P_1 \rightarrow {}^1S_0$ transition, owing to Bi^{3+} ions have been observed. PL spectra revealed that the phosphors with Gd – containing host has exhibited a better luminescence among the others. The luminescence intensity sequence in descending order was as follows: $GdVO_4 \rightarrow (Gd, Y)VO_4 \rightarrow (La, Gd)VO_4 \rightarrow (La, Y)VO_4 \rightarrow YVO_4 \rightarrow LaVO_4$: Bi^{3+}. These phosphors can efficiently convert the UV-photons in a broad range from 280–350 nm of feckless UV-rays into the absorbable visible emission for c-Si solar cells, based on the spectral matching phenomena. In view of the better fluorescence and pertinent optical properties, the phosphor with composition $Gd_{0.97}VO_4$: $Bi^{3+}_{0.03}$ is a suggestible sought UV-absorbing spectral converter, in its thin transparent DC form for c-Si solar cells for better harvesting the solar energy.

Keywords: A: Chemical preparation; B: Composites; C: Optical properties

1. Introduction

In order to solve the problem of energy crisis, it is necessary to explore the promising application of green and sustainable energy. As a result solar energy has received more attention in recent years. At present, the solar photovoltaic (PV) technology is one of the major attempts to harness the solar energy. However, the PV conversion efficiency is still not high enough to compete with the fossil fuels and nuclear energy. The attempt to improve the PV conversion efficiency is still under investigation. The efficiency of single band-gap solar cell is constrained by matching the systems band-gap to the radiation spectrum of the sun. The Shockley–Queasier limit [1] of 31% for a single junction semiconductor soar cell is possible for a material with a band-gap of 1.1–1.3 eV, in the range of many common semiconductors such as Silicon (Si) and Gallium Arsenide (GaAs) [2]. Moreover, with a single junction solar cell not all the irradiated solar energy is utilized, some of the energy will be lost by lower energy photons that are transparent to semiconductor, and an additional portion is lost as thermalization of higher energy photons. These losses have been added up to more than 50% of the utilizable solar energy for a Si solar cell [3]. Various concepts have been proposed over the past few years to overcome this fundamental efficiency limit for a single junction solar cell [4,5]. These concepts include as multi junction solar cells, inter-band transitions and recently introduced up, down-conversion models [5].

Down-conversion (DC) is intended to better utilize the free energy of photons with energy higher than the band-gap of solar cell, which is otherwise loss to thermalization. In the DC process first analyzed by Trupke et al. [6–8], an

*Corresponding author. Tel.: +82428603449.
E-mail address: sdhan@kier.re.kr (S.-D. Han).

0272-8842/$36.00 © 2012 Elsevier Ltd and Techna Group S.r.l. All rights reserved.
http://dx.doi.org/10.1016/j.ceramint.2012.06.081

individual luminescent material placed in front of the solar cell will be used to split the photons with energy at twice the band-gap energy into two lower energy photons, which are better matched to the solar cells band gap. DC is proposed to increase the current of the solar cell by increasing the number of absorbed photons impinging upon the solar cell while retaining its voltage characteristics. This increase in current subsequently increases the overall efficiency of the cell system. The strongest emission of the solar spectrum is around 350–550 nm, the energy which is twice as high as the energy gap of crystalline silicon ($E_g = 1.12$ eV, $\lambda = 1100$ nm). An ideal way to achieve DC is the energy transfer by using rare earth (RE) ions. The unique and rich energy level structure of RE ions allows for efficient spectral modification, by energy transfer of neighboring RE ions [9]. The trivalent lanthanide ions (Ln^{3+}) with abundant energy levels arising from the 4f inner shell configuration suited for spectral conversion in solar cells. Recently, more attention has been paid to YVO_4 host phosphors, especially as DC phosphors for dye sensitized solar cells (DSSCs), because it has many remarkable characteristics including good thermal, mechanical and optical properties [10]. The experimental band gap of YVO_4 is 3.8 eV, whereas substitution of Y^{3+} ions with Bi^{3+} ions could result in a significant reduction in the band gap [11–15]. From the literature to the best of our knowledge, it is understood that there are hardly any report available on the study of the effect of host composition on luminescence intensity with Bi-doped lanthanide vanadate phosphors, in tuning the better phosphor composition as DC phosphors.

In the present work, we have focused our attention on the effect of single and dual lanthanide vanadate host on fluorescence and pertinent optical properties of Bi^{3+} -doped vanadate phosphors. The proposed phosphors are synthesized by a simple and commercially viable co-precipitation technique followed by heat-treatment. Produced, $LnVO_4$ and (Ln1, Ln2)VO_4: Bi^{3+} phosphors are proposed to be the promising UV-absorbing spectral converters for c-Si solar cells. As they possess a broad band absorption in the UV-region of 280–350 nm and could able to emit in a broad visible greenish-yellow region.

2. Experimental procedure

2.1. Synthesis of $Ln_{0.97}VO_4$: $Bi^{3+}_{0.03}$ and $(Ln1_{0.5}, Ln2_{0.5})_{0.97}VO_4$: $Bi^{3+}_{0.03}$ (where Ln=La, Gd and Y) powder phosphors

For the synthesis of the proposed Bi doped single and dual host vanadate phosphors, a co-precipitation technique, followed by calcination was adopted. Where the starting precursors were supposed to react at micro level and lead to homogeneous better product. As we know that different material preparation techniques may have some important effects on material microstructure, physical, optical and luminescence properties [16]. Based on our previous studies (data under publication), an optimum dopant bismuth concentration was fixed as 0.03 mol.

Yttrium nitrate ($Y(NO_3)_3.6H_2O$) (99.99%, Aldrich make), gadolinium nitrate ($Gd(NO_3)_3.6H_2O$) (99.99%, Aldrich make), lanthanum nitrate ($La(NO_3)_3.6H_2O$) (99.99%, Aldrich make), bismuth oxide (Bi_2O_3)(99.99%, Aldrich make), ammonium metavanadate (NH_4VO_3) (99+%, Aldrich make), ethylene di-amine tetra acetic acid disodium salt dihydrate ($C_{10}H_{16}N_2O_8$)(EDTA)(99+%, Aldrich make), ethylene glycol (99.99%, Aldrich make), nitric acid (98%) and ammonia (NH_3) solution (assay 28–30%,) were used as the precursors. Initially, lanthanide nitrates, Bi_2O_3 and NH_4VO_3 were dissolved in dilute nitric acid with stirring and moderate heating on a hot plate. Ammonium metavanadate was used as a vanadate source. After the complete dissolution an equal volume of IM EDTA solution was added to the above resultant solution as a metal to metal chelating agent, under vigorous stirring. A certain amount of ethylene glycol was also added as a surfactant media. The pH of the final solution was maintained as 9.0 with NH_4OH, under vigorous stirring with drop wise addition. A slightly yellow colour precipitate was formed, which was allowed to stir for minimum one hour. The obtained precipitate was washed thoroughly with ethanol and D.I water, in order to remove the unreacted remnants and traces of solvents. Further, it was dried in an electric oven at 120 °C. The dried powders were crushed in an agate mortar and pre-heated from room temperature to 700 °C for 2 h. Simultaneously, the temperature was increased to 1000 °C and kept for 3 h in order to get better crystalinity and intense luminescence. Both the single and dual lanthanide vanadates with bismuth dopant were prepared in a similar fashion, according to their stoichiometric ratios.

2.2. Characterization

The crystalinity and phase purity of the synthesized powder phosphors are investigated by X-ray Diffraction (XRD), using Rigaku X-ray Diffractometer D/max 2500 ultima having CuK_α radiation ($\lambda = 1.5406$ Å) at 40 kV tube voltage and 40 mA tube current. The XRD patterns were measured with diffraction angle (2Θ) ranging, $15^\circ \leq 2\Theta \leq 70^\circ$. Photoluminescence (PL) of the produced phosphors was measured with a Minolta Spectroradiometer, CS-1000. Before, measuring ~5 g of phosphor sample was spread onto a flat surface of 50 mm diameter and 1 mm thickness. A 365/312 nm UV lamp mounted on top of the sample with certain height was used as an excitation source. The PL measurements were carried out at room temperature with the wavelength region 400–700 nm. The chromaticity coordinates (x, y) as per Commission International de E'Clarage (CIE), were measured using the same set-up of Minolta Spectroradiometer. The PL spectra were also measured by using Scinco spectroflurometer with photomultiplier tube voltage 500, integration time 20 ms, excitation slit 5 nm and emission slit 5 nm. The surface morphology,

crystallite size and qualitative elemental analysis of the synthesized phosphors were studied using Hitachi, S-4700 Scanning Electron Microscope (SEM) with Horiba EDS attachment. The measurement conditions like accelerating voltage (kV), working distance (mm), magnification (x K) and scale bar employed for each sample were available on micrographs. The chemical bonding/functional group details of the prepared phosphors are measured using, Shimadzu 8900, Fourier Transform-Infrared (FT-IR) spectrometer with potassium bromide (KBr) pellet technique. The FT-IR spectral measurements were carried out in the wavenumber region 400–4000 cm^{-1}.

3. Results and discussion

Fig. 1 shows the XRD patterns of: (a) $Y_{0.97}VO_4$: $Bi^{3+}_{0.03}$, (b) $(Gd_{0.5}, Y_{0.5})_{0.97}VO_4$: $Bi^{3+}_{0.03}$, (c) $(La_{0.5}, Y_{0.5})_{0.97}VO_4$: $Bi^{3+}_{0.03}$, (d) $Gd_{0.97}VO_4$: $Bi^{3+}_{0.03}$, (e) $La_{0.97}VO_4$: $Bi^{3+}_{0.03}$ and (f) $(La_{0.5}, Gd_{0.5})_{0.97}VO_4$: $Bi^{3+}_{0.03}$, powder phosphors. The XRD profile of $Y_{0.97}VO_4$: $Bi^{3+}_{0.03}$ (Fig. 1a) has shown to be well matched with the JCPDS file No: 72-0861. It has tetragonal phase with body centered, where the cell parameters are: $a=7.123$ and $c=6.292$. Even with the substitution of Y^{3+} with Bi^{3+} ions, there was no any notable change in the major diffraction peak positions: (101), (200), (220), (301), (321), (312) and (400). No additional diffraction peaks that could be attributed to impurity phases were observed, indicating that an appreciable amount of Bi^{3+} doping to host matrix has does not altered the host structure, YVO_4. The XRD profile of $Gd_{0.97}VO_4$:$Bi^{3+}_{0.03}$ (Fig. 1d) is in good agreement with the JCPDS file No: 170260. It has shown tetragonal phase with body centered, where the cell parameters are: $a=7.212$ and $c=6.348$. There was no any appreciable shift in the major diffraction peak positions of (101), (200), (112), (220) and (312), even with the substitution of Gd^{3+} with Bi^{3+}. Similarly, the XRD profile of $La_{0.97}VO_4$: $Bi^{3+}_{0.03}$ (Fig. 1e) has also well agreed with the JCPDS file No: 702392. It has monoclinic phase with cell parameters: $a=7.038$, $b=7.269$, $c=6.719$ and $\beta=104.91$. No appreciable shift in the major diffraction peaks of (020), (200), (120), (012) and (132) were noted, even with the fractional substitution of La^{3+} to Bi^{3+}. From the XRD profiles of $(Gd_{0.5}, Y_{0.5})_{0.97}VO_4$: Bi^{3+} (Fig. 1b) and $(La_{0.5}, Y_{0.5})_{0.97}VO_4$:$Bi^{3+}$ (Fig. 1c), it is revealed that the individual crystal structures of Gd and La-vanadates were dominated by the crystal structure of YVO_4, i.e. body centered tetragonal phase, with their additional presence of weak individual diffraction peaks, with minor shifts in the major peak positions, as illustrated in Fig. 1. Similarly, the crystal structure of $(La_{0.5}, Gd_{0.5})_{0.97}VO_4$: Bi^{3+} is also has tetragonal phase of $GdVO_4$ by dominating the monoclinic phase of $LaVO_4$, however with the weak presence of $LaVO_4$ diffraction peaks, additionally. The doped Bi^{3+} ions might occupy the Ln^{3+} sites, owing to their nearby ionic radii (Y^{3+}, $r=0.09$ nm, La^{3+}, $r=0.10$ nm, Gd^{3+}, $r=0.093$ and Bi^{3+}, $r=0.103$ nm). The evidence for the substitution of Bi^{3+} ions with lanthanide ions was confirmed by EDAX and PL measurements [15–17].

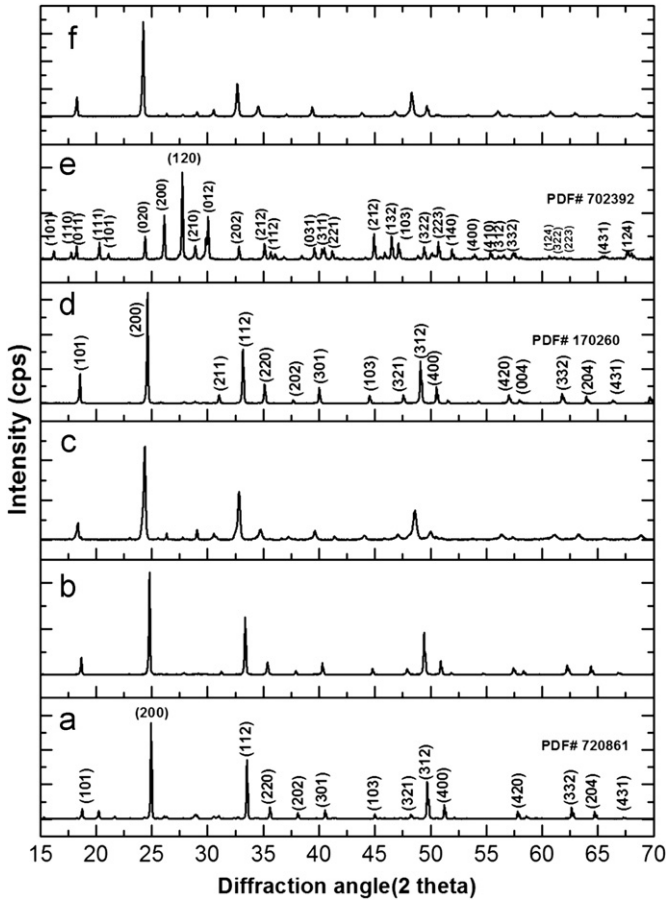

Fig. 1. XRD patterns of (a) $Y_{0.97}VO_4$:$Bi^{3+}_{0.03}$, (b) $(Gd_{0.5}, Y_{0.5})_{0.97}VO_4$: $Bi^{3+}_{0.03}$, (c) $(La_{0.5}, Y_{0.5})_{0.97}VO_4$:$Bi^{3+}_{0.03}$, (d) $Gd_{0.97}VO_4$:$Bi^{3+}_{0.03}$, (e) $La_{0.97}VO_4$:-$Bi^{3+}_{0.03}$and (f) $(La_{0.5}, Gd_{0.5})_{0.97}VO_4$:$Bi^{3+}_{0.03}$, powder phosphors.

Fig. 2 shows the SEM images of: (a) $La_{0.97}VO_4$: $Bi^{3+}_{0.03}$, (b) $Y_{0.97}VO_4$: $Bi^{3+}_{0.03}$, (c) $Gd_{0.97}VO_4$: $Bi^{3+}_{0.03}$ and (d) $(Gd_{0.5},Y_{0.5})_{0.97}VO_4$: $Bi^{3+}_{0.03}$, powder phosphors. From the SEM micrographs it is obvious that the synthesized powder phosphors are having the crystallite size in the range 350 nm to 13 μm with an irregular shape.

Fig. 3 (a, b) shows the Energy Dispersive X-ray Analysis (EDAX) spectra of (a) $Gd_{0.97}VO_4$: $Bi^{3+}_{0.03}$ and (b) $(Gd_{0.5},Y_{0.5})_{0.97}VO_4$: $Bi^{3+}_{0.03}$, powder phosphors. The EDAX spectra elucidate the qualitative analysis of the elements: Gd, Y, V, O, and Bi, present in the samples. Moreover, it clarifies that the samples does not contain any other elements as impurities. A possible chance for added up from the precursors during precipitation process.

Fig. 4 shows the FT-IR spectra of (a) $La_{0.97}VO_4$: $Bi^{3+}_{0.03}$ and (b) $(Gd_{0.5}, Y_{0.5})_{0.97}VO_4$: $Bi^{3+}_{0.03}$ powder phosphors, measured in the frequency region 400–4000 cm^{-1}. Modes in the region observed are due to the vanadium–oxygen (V–O) stretching vibrations of $[VO_4]^{3-}$ and the other M–O (M=Y, Gd, La and Bi) bonds present in the phosphors. The weak, but an intense signals of M–O bond was found to be at around 438, 592 & 775 cm^{-1} in the case of $LaVO_4$ host, the same peaks measured at 450, 610 and 769 cm^{-1},

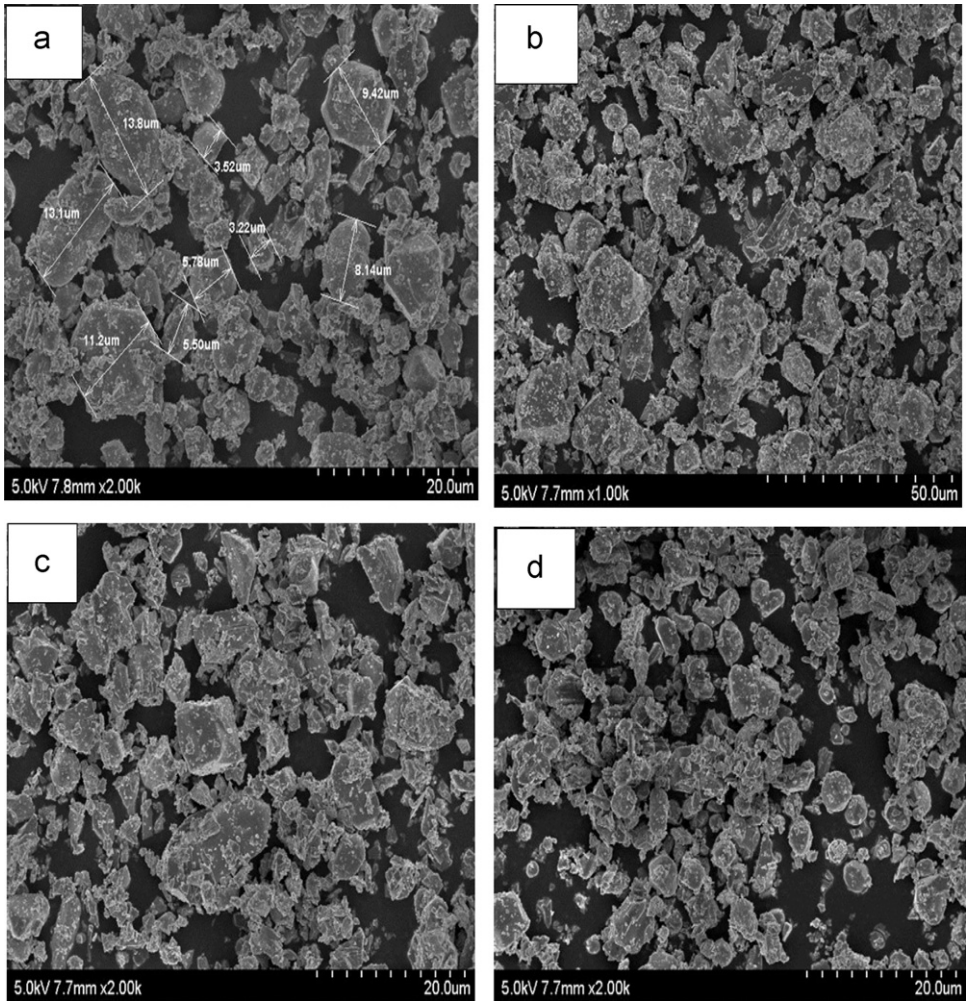

Fig. 2. SEM images of (a) $La_{0.97}VO_4:Bi^{3+}_{0.03}$, (b) $Y_{0.97}VO_4:Bi^{3+}_{0.03}$, (c) $Gd_{0.97}VO_4:Bi^{3+}_{0.03}$, and (d) $(Gd_{0.5}, Y_{0.5})_{0.97}VO_4:Bi^{3+}_{0.03}$, powder phosphors.

in the case of dual lanthanide hosts such as (Gd, Y)VO_4. An intense and broad absorption peak in the wavenumber region 500–1000 cm^{-1} with its centre at 769 cm^{-1} with shoulder at 947 cm^{-1} for $La_{0.97}VO_4$: $Bi^{3+}_{0.03}$ and at 837 cm^{-1} with shoulder at 954 cm^{-1} for $(Gd_{0.5},Y_{0.5})_{0.97}VO_4$: $Bi^{3+}_{0.03}$, attributed to the V–O (from VO_4^{3-} group) stretching mode. The appreciable shift towards higher wavenumber side might be due to the influence of the dual lanthanides in the host matrix. The peaks due to O–H stretching vibration and H–O–H bending vibrational modes owing to absorption of moisture on the surface of the powders as reported by the other researchers for vanadate phosphors have not been observed in case of our samples [15,18–21]. Furthermore, the FT-IR spectral measurement certifies the vanadate phase formation, agreeing well with the obtained XRD, results.

Fig. 5 shows the excitation spectra of the phosphors (a) $Y_{0.97}VO_4$: $Bi^{3+}_{0.03}$, (b) $Gd_{0.97}VO_4$: $Bi^{3+}_{0.03}$, (c) $La_{0.97}VO_4$: $Bi^{3+}_{0.03}$, (d) $(La_{0.5}, Y_{0.5})_{0.97}VO_4$: $Bi^{3+}_{0.03}$, (e) $(La_{0.5}, Gd_{0.5})_{0.97}VO_4$: $Bi^{3+}_{0.03}$ and (f) $(Gd_{0.5}, Y_{0.5})_{0.97}VO_4$: $Bi^{3+}_{0.03}$, monitored with $\lambda_{em}=550$ nm. It is obvious from the spectra that it has a broad absorption band with its centre at around 330–340 nm in the wavelength region 280–350 nm. The strong broad excitation band is due to the absorption of Bi^{3+}, ions. These ions have an outer $6s^2$ electronic configuration with ground state of $^1S_0$, the excited states have 6s6p configuration and are split into the $^3P_0$, $^3P_1$, $^3P_2$ and $^1S_1$, levels in sequence of increasing energy. Transitions between $^1S_0$ and $^3P_0$, $^3P_1$ or $^3P_2$ are spin forbidden, however, the $^3P_1$ level undergoes mixing with $^1P_1$ by spin-orbit coupling, allowing the $^1S_0 \rightarrow {}^3P_1$ transitions that are frequently observed in PL measurements. As per the literature, we consider that the strong broad excitation band at 330–340 nm is ascribed to $^1S_0 \rightarrow {}^3P_1$, transition of Bi^{3+}, ions [22–27]. It can be seen from the excitation spectra that the intensity and wavelength of the excitation band $^1S_0 \rightarrow {}^3P_1$ are found to be varied with the host composition, even the dopant Bi^{3+}-ions concentration was fixed as 0.03 mol. The absorption band shift is ascribed to the charge transfer process in the excited state of Bi^{3+}, ions. Jamila et al [28], have explained that the position of the absorption bands does not depend on the structure of the lattice, but rather upon the local field experienced by the Bi^{3+} ions ($6S^2$) in the host environment. Special attention might be required to focus on the effects of changing the internal pressure on the Bi ions

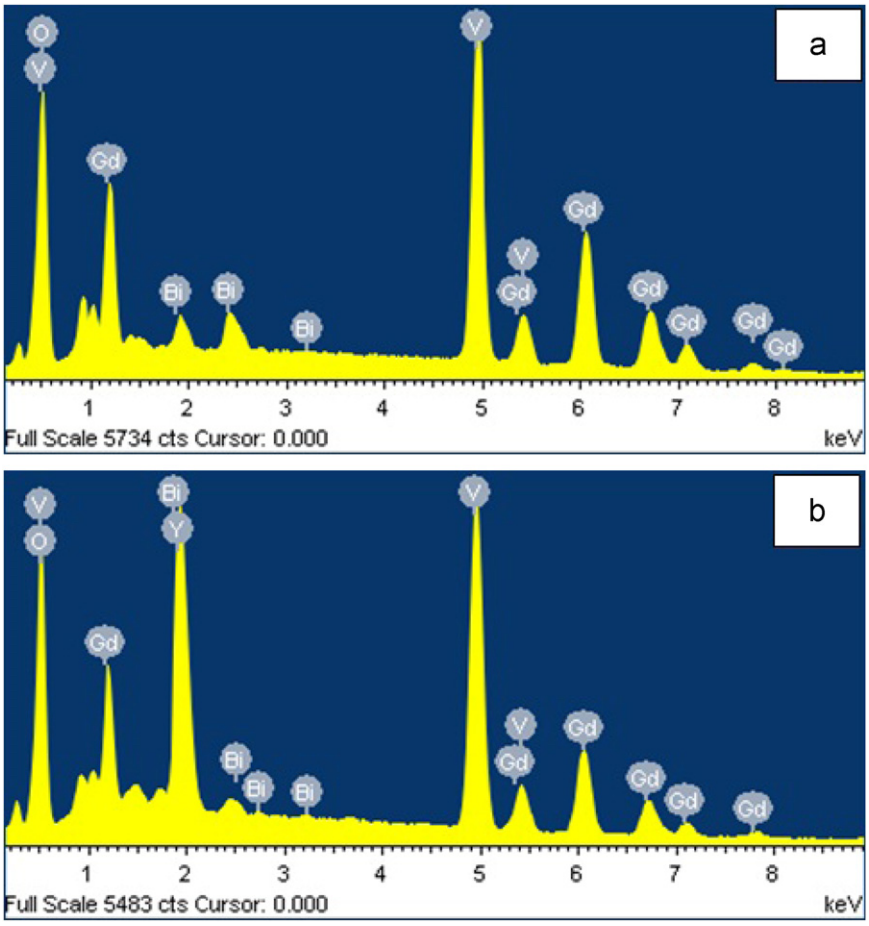

Fig. 3. Energy Dispersive X-ray Analysis (EDAX) spectra of (a) $Gd_{0.97}VO_4:Bi^{3+}_{0.03}$ and (b) $(Gd_{0.5}, Y_{0.5})_{0.97}VO_4:Bi^{3+}_{0.03}$, powder phosphors.

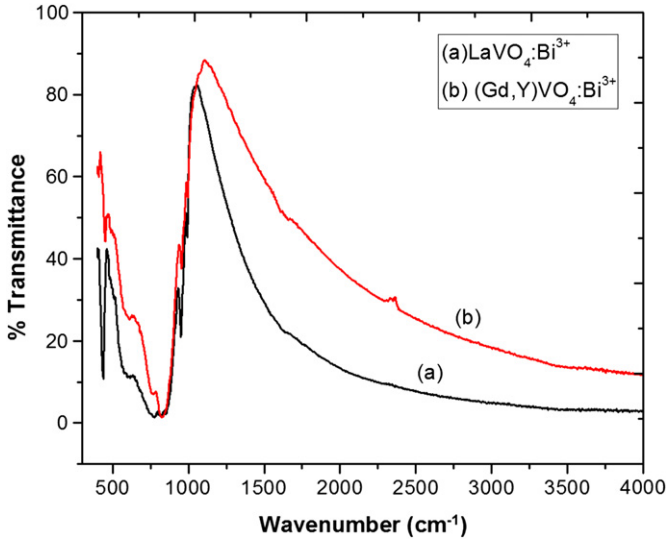

Fig. 4. FT-IR spectra of (a) $La_{0.97}VO_4:Bi^{3+}_{0.03}$ and (b) $(Gd_{0.5}, Y_{0.5})_{0.97}VO_4:Bi^{3+}_{0.03}$, powder phosphors.

which strongly influence the Bi^{3+} absorption or emission band. Indeed, these bands may be located in the spectral range lying from ultra violet (UV) to infrared (IR) region [28].

Fig. 6 (I) shows the photoluminescence spectra of the phosphors: (a) $Y_{0.97}VO_4$: $Bi^{3+}_{0.03}$, (b) $Gd_{0.97}VO_4$: $Bi^{3+}_{0.03}$, (c) $La_{0.97}VO_4$: $Bi^{3+}_{0.03}$, (d) $(La_{0.5}, Y_{0.5})_{0.97}VO_4$: $Bi^{3+}_{0.03}$, (e) $(La_{0.5}, Gd_{0.5})_{0.97}VO_4$: $Bi^{3+}_{0.03}$ and (f) $(Gd_{0.5}, Y_{0.5})_{0.97}VO_4$: $Bi^{3+}_{0.03}$, monitored with the excitation wavelengths as mentioned in the figure. These phosphors consist of a broad emission band centered at 543–550 nm, ascribed to the transition of Bi^{3+}; $^3P_1 \rightarrow {}^1S_0$. A small blue peak observed at 460 nm was originated from the energy transition of molecular or orbital $[VO_4]^{3-}$ group, which is in good agreement with the literature reports [29,30].

From the emission spectra it is revealed that the intensity and peak position of the broad band $^3P_1 \rightarrow {}^1S_0$, are observed to be varied with the host composition of the lanthanide ions used. PL spectra elucidates that the phosphors with gadolinium content have shown better luminescence intensities compared with the others. The phosphor with chemical composition, $Gd_{0.97}VO_4$: $Bi^{3+}_{0.03}$ has exhibited a maximum PL intensity among the synthesized phosphors, even though these host lanthanides consist nearby ionic radius (Y^{3+}, $r=0.09$ nm, La^{3+}, $r=0.10$ nm, Gd^{3+}, $r=0.093$ and Bi^{3+}, $r=0.103$ nm). Generally, in luminescent materials, phosphors based on gadolinium compounds play an important role because the Gd^{3+} ion ($4f^7$, ^8S) has its lowest excited levels at relatively

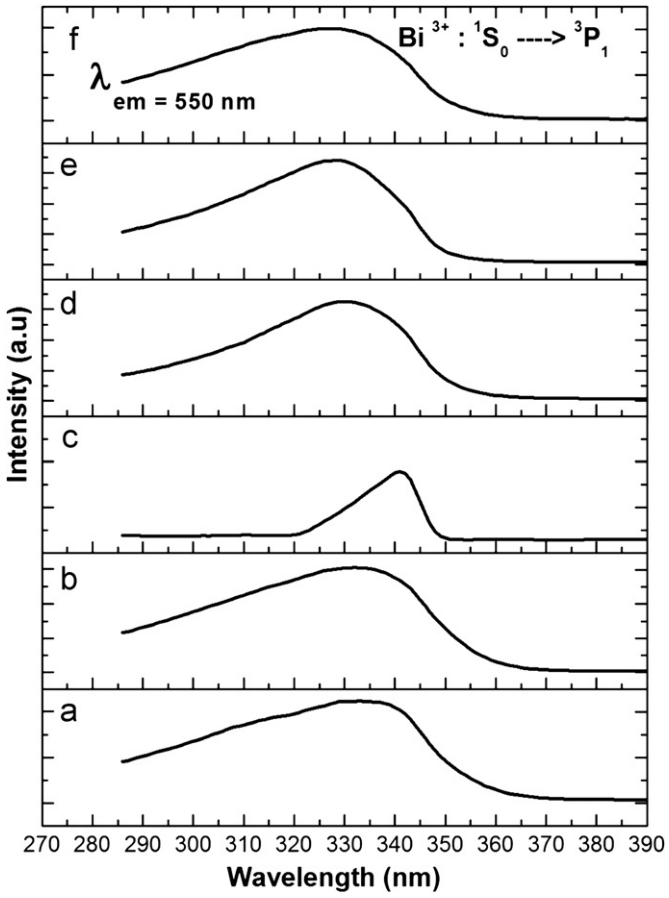

Fig. 5. Excitation spectra of the phosphors (a) $Y_{0.97}VO_4:Bi^{3+}_{0.03}$, (b) $Gd_{0.97}VO_4:Bi^{3+}_{0.03}$, (c) $La_{0.97}VO_4:Bi^{3+}_{0.03}$, (d) $(La_{0.5}, Y_{0.5})_{0.97}VO_4:Bi^{3+}_{0.03}$, (e) $(La_{0.5}, Gd_{0.5})_{0.97}VO_4:Bi^{3+}_{0.03}$ and (f) $(Gd_{0.5}, Y_{0.5})_{0.97}VO_4:Bi^{3+}_{0.03}$, monitored at $\lambda_{em}=550$ nm.

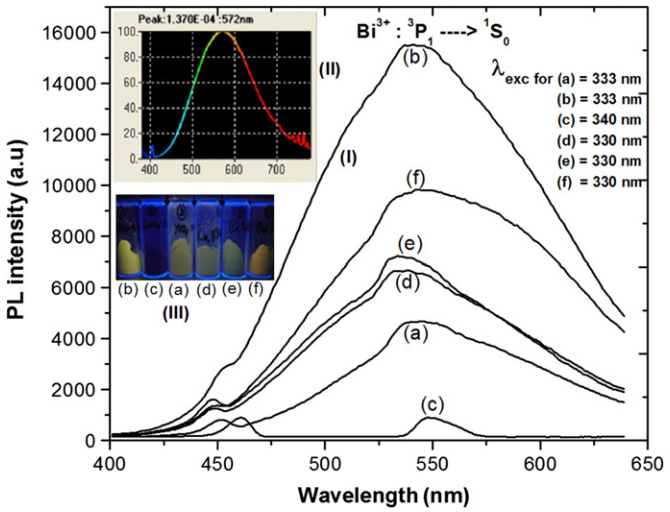

Fig. 6. (I) Photoluminescence spectra of the phosphors: (a) $Y_{0.97}VO_4:Bi^{3+}_{0.03}$, (b) $Gd_{0.97}VO_4:Bi^{3+}_{0.03}$, (c) $La_{0.97}VO_4:Bi^{3+}_{0.03}$, (d) $(La_{0.5}, Y_{0.5})_{0.97}VO_4:Bi^{3+}_{0.03}$, (e) $(La_{0.5}, Gd_{0.5})_{0.97}VO_4:Bi^{3+}_{0.03}$ and (f) $(Gd_{0.5}, Y_{0.5})_{0.97}VO_4:Bi^{3+}_{0.03}$, monitored at the excitation wavelengths as mentioned in the figure. (II) PL spectrum of the phosphor $Gd_{0.97}VO_4:Bi^{3+}_{0.03}$, measured with Spectroradiometer and (III) Photograph shows the greenish-yellow emission from the above phosphors (a→f), upon 312 nm UV-source excitation. (For interpretation of the references to color in this figure legend, the reader is referred to the web version of this article.)

high energy due to the stability of the half-filled shell ground state [31,32].

Fig. 6 (II) shows the PL spectrum of the phosphor, $Gd_{0.97}VO_4$: $Bi^{3+}_{0.03}$ recorded with Spectroradiometer, with the aid of 312 nm UV lamp, by spreading the sample as a thick film, as explained in the experimental part. An intense broad band emission observed from 400–700 nm with centre at 572 nm is ascribed to Bi^{3+}; $^3P_1 \rightarrow {}^1S_0$, indicates an intense greenish-yellow emission. This was confirmed by the photograph as shown in Fig. 6(III), upon 312 nm UV-irradiation. From Fig. 6(II), a group of small peaks observed above 700 nm are due to noise level, we normally noted for all the samples, measured with Minolta Spectroradiometer.

The quality and colour richness of the produced phosphors are checked by measuring the colour coordinates (x,y), by using Minolta Spectroradiometer with the aid of 312 nm UV-lamp. The obtained x,y–colour coordinates are well fitted in the yellowish-green region of the Commission International de'Eclairage (CIE), chromaticity diagram, except for the phosphor, i.e. $La_{0.97}VO_4:Bi^{3+}$ which has found to be fitted in the blue/hue region as shown in the Fig. 7. The reason for the phosphor $La_{0.97}VO_4:Bi^{3+}$ to

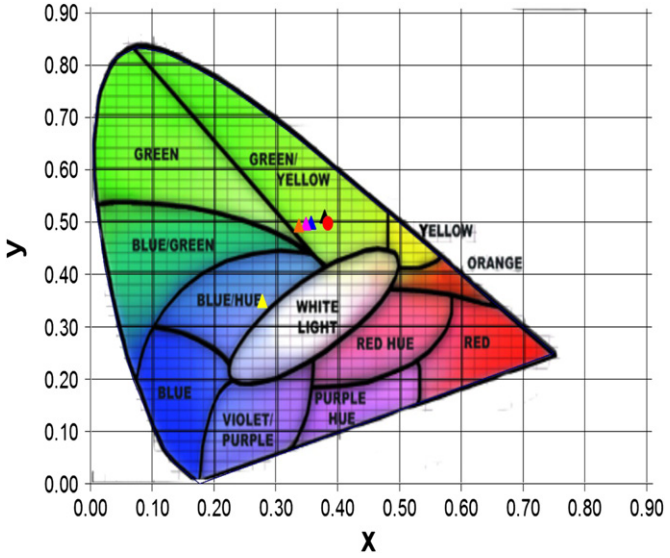

Fig. 7. CIE, chromaticity diagram, where the obtained colour coordinates (x,y) are well fitted in the greenish-yellow region except $La_{0.97}VO_4:Bi^{3+}_{0.03}$, which was fitted in the blue/hue region. (For interpretation of the references to color in this figure legend, the reader is referred to the web version of this article.)

occupy blue/hue region could be its weak PL luminescence intensity compared with the other phosphors as shown in the PL spectra of Fig. 6(ii).

Fig. 8 shows the schematic energy level diagram of Bi^{3+} in $LnVO_4$ (Ln=La, Gd and Y) host, phosphors. Solid arrows represent allowed transitions and dashed lines are forbidden transitions. Bi^{3+} ions have an outer $6S^2$ electronic configuration. Its ground state is a spin-orbit singlet

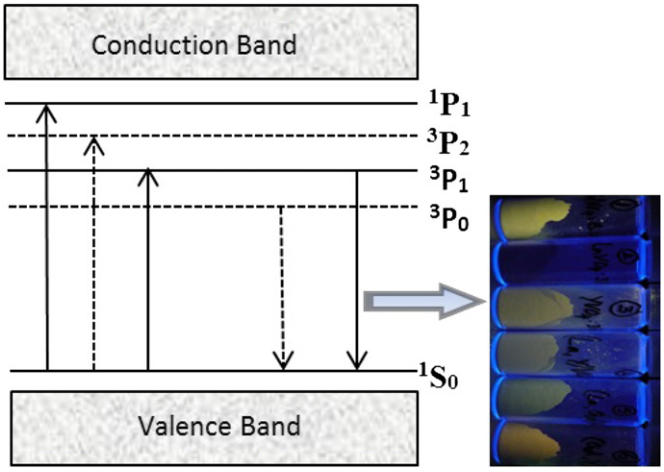

Fig. 8. Schematic energy level diagram of $LnVO_4$: Bi^{3+} (Ln=La, Gd and Y) powder phosphors. Solid arrows represent allowed transitions and dashed one is forbidden.

($^1S_0$). The excited state has 6s6p configuration. The lower state with spin parallel (6s6p) yields a lower 3P state. This state splits into $^3P_0$, $^3P_1$, and $^3P_2$ levels in a sequence of increasing energy due to the spin-orbit interaction. The next higher excited state $^1P_1$ is an inter-configuration transition and both parity and spin allowed while the $^1S_0 \rightarrow {}^3P_2$ transition is spin forbidden [33]. It is obvious that these phosphors are excited with high energy UV rays (330–340 nm) and emitted at nearly double the wavelength as lower energy photons, in the visible greenish-yellow region. As per the down conversion phenomena, the absorbed high energy photons in the UV region where the c-Si solar cell is not able to absorb are emitted by splitting into Si-solar cell acceptable lower energy photons at greenish-yellow visible region, as per the spectral matching concept. Thus, based on the obtained luminescence and pertinent optical properties, the phosphor with chemical composition $Gd_{0.97}VO_4$: $Bi^{3+}_{0.03}$, could be a remarkable contender as a DC phosphor for its further research in order to fabricate it in a transparent thin film form. Towards its use as a mask layer of the c-Si solar cells in view of better harvesting the solar spectrum in terms of power conversion efficiency. In a continuation, we are in the process of fabricating a thin transparent film of $Gd_{0.97}VO_4$: Bi^{3+} by embedding these phosphor powders in ethylene vinyl acetate (EVA) co-polymer and to demonstrate its performance as a DC layer towards its power conversion efficiency over a virgin c-Si solar cell.

4. Conclusions

In summary, it is concluded that $Ln_{0.97}VO_4$: $Bi^{3+}_{0.03}$ and $(Ln1_{0.5}, Ln2_{0.5})_{0.97}VO_4$: $Bi^{3+}_{0.03}$ (where Ln=La, Gd & Y) powder phosphors have been successfully synthesized by a simple co-precipitation technique. XRD investigation revealed that in the case of dual lanthanide (La, Gd & Y) vanadate host phosphors the crystal structure of YVO_4, $GdVO_4$ (tetragonal phase with body centered) has dominated the crystal structure of $LaVO_4$ (monoclinic phase). The vanadate phase formation of the produced phosphors was reconfirmed by FT-IR spectra, evidenced by V–O and M–O (M=Y, La, Gd & Bi) vibrational bands. A broad band excitation assigned to $^1S_0 \rightarrow {}^3P_1$ and an intense broad greenish-yellow-band (400–700nm) ascribed to $^3P_1 \rightarrow {}^1S_0$ transition, owing to Bi^{3+} was observed. The measured color coordinates (x,y) are well fitted in the greenish-yellow region of the CIE, chromaticity diagram. PL spectra elucidate that the phosphors with Gd-based host exhibited better luminescence among the others. The luminescence intensity sequence of the synthesized phosphors in descending order was as follows: $GdVO_4 \rightarrow (Gd,Y)VO_4 \rightarrow (La,Gd)VO_4 \rightarrow (La,Y)VO_4 \rightarrow YVO_4 \rightarrow LaVO_4$: Bi^{3+}. As per the down conversion phenomena, these phosphors have excited with high energy UV-rays (330–340 nm) and emitted nearly at double the wavelength as lower energy photons, in the visible greenish-yellow region, as Si-solar cell absorbing radiation. Based on the luminescence and pertinent optical properties, the phosphor $Gd_{0.97}VO_4$: $Bi^{3+}_{0.03}$, could be suggested as a sought DC-phosphor candidate for its further research, in its transparent thin film form for c-Si solar cells for better harvesting the solar spectrum, in enhancing the power conversion efficiency of a virgin Si-solar cell. This research may focus the light on the search for promising new techniques for the fabrication of thin and transparent films out of this optimized DC phosphor towards its application in c-Si solar cells.

Acknowledgments

One of the authors, URB would like to thank Korean Federation of Science and Technology (KOFST), Korea for awarding Brain pool Fellowship and also express his gratitude to Dr. T. L. Prakash, Director and Dr. D. P. Amalnerkar, Executive Director of C-MET, Pune for allowing to carry this research work at Korea Institute of Energy Research (KIER), Korea.

References

[1] S. William, J.Q. Hans, Detailed balance limit of efficiency of *p–n* junction solar cells, Journal of Applied Physics 32 (1962) 510–520.
[2] R.A. Zeev, N. Avi, Z. Xiang, Solar energy enhancement using down-converting particles: a rigorous approach, Journal of Applied Physics 109 (2011) 114905-1–114905-9.
[3] A. Wolf, A new look at silicon solar cell performance, Energy Conversion 11 (1971) 63–73.
[4] A. Wolf, Limitations and possibilities for improvement of photovoltaic solar energy converters: part I: considerations for earth's surface operation, Proceedings of the Institute of Radio Engineers 48 (1960) 1246–1263.
[5] M.A. Green, Third Generation Photovoltaic, Springer-Verlag, Berlin, 2003.
[6] T. Trupke, M.A. Green, P. Würfel, Improving solar cell efficiencies by down-conversion of high-energy photons, Journal of Applied Physics 92 (2002) 1668–1675.
[7] V. Badescu, A. De Vos, A.M. Badescu, A. Szymanska, Improved model for solar cells with down-conversion and down-shifting of

high-energy photons, Journal of Physics D: Applied Physics 40 (2007) 341–346.
[8] V. Badescu, A. De Vos, Influence of some design parameters on the efficiency of solar cells with down-conversion and down shifting of high-energy photons, Journal of Applied Physics 102 (2007) 073102-1–073102-7.
[9] C. Xuerui, S. Lei S, W. Yongquang, Z. Xiang, W. Xiantao, W. Yuyin, Near-infrared quantum cutting in YVO_4: Yb^{3+} thin-films via down conversion, Optical Materials (2012). http://dx.doi.org/10.1016/j.optmat.2012.01.014.
[10] X.Y. Huang, J.X. Wang, D.C. Yu, S. Ye, Q.Y. Zhang, X.W. Sun, Spectral conversion for solar cell efficiency enhancement using YVO_4: Bi^{3+}, Ln^{3+} (Ln=Dy, Er, Ho, Eu, Sm and Yb) phosphors, Journal of Applied Physics 109 (2011) 113526-1-7.
[11] M.R. Doglos, A.M. Paraskos, M.W. Stoltzfus, S.C. Yarnell, P.M. Woodward, The electronic structure of vanadate salts: cation substitution as a tool for band gap manipulation, Journal of Solid State Chemistry 182 (2009) 1964–1971.
[12] M.W. Stoltzfus, P.M. Woodward, R. Seshadri, J. Klepeis, B. Bursten, Structure and bonding in $SnWO_4$, $PbWO_4$, and $BiVO_4$: lone pairs vs. inert pairs, Inorganic Chemistry 46 (2007) 3839–3850.
[13] S. Neeraj, N. Kijima, A.K. Cheetham, Novel red phosphor for solid state lighting; the system Bi_x $Ln_{1-x}VO_4$: Eu^{3+}/Sm^{3+} (Ln=Y, Gd), Solid State Communications 131 (2004) 65–69.
[14] S. Takeshita, H.T. Ogata Isobe, T. Sawayama, S. Niikura, Effects of citrate additive on transparency and photo stability properties of YVO_4: Bi^{3+}, Eu^{3+} nanophosphor, Journal of Electrochemical Society 157 (2010) J74–J80.
[15] Z.G. Xia, D.M. Chen, M. Yang, T. Ying, Synthesis and luminescence properties of YVO_4: Eu^{3+}, Bi^{3+} phosphor with enhanced photoluminescence by Bi^{3+} doping, Journal of Physical Chemistry of Solids 71 (2010) 175–180.
[16] L. Chen, G. Liu, Y. Liu, K. Huang, Synthesis and luminescence properties of YVO_4: Dy^{3+} nanorods, Journal of Materials Process Technology 198 (2008) 129–133.
[17] L. Jihong, L. Jie, Y. Xibin, Synthesis and luminescence properties of Bi^{3+} doped YVO_4 phosphors, Journal of Alloys and compounds 509 (2011) 9897–9900.
[18] L. Xue, Y. Min, H. Zhiyao, L. Guogang, M. Pingan, W. Wenxin, C. Ziyong, L. Jun, One dimensional $GdVO_4$: Ln^{3+} (Ln=Eu, Dy, Sm) nanofibers: Electrospinning preparation and luminescence properties, Journal of Solid State Chemistry 184 (2011) 141–148.
[19] B.V. Rao, G.B. Kumar, M. Jayasimhadri, K. Jang, H.S. Lee, S.S. Yi, J.H. Jeong, Photoluminescence and spectral properties of $Ca_3Y(VO_4)_3$: RE^{3+}(= Sm^{3+}, Ho^{3+} & Tm^{3+}) powder phosphors for tricolours, Journal of Crystal Growth 326 (2011) 120–123.
[20] G. Liu, X. Duan, H. Li, H. Dong, Hydrothermal synthesis, characterization and optical properties of novel fishbone like $LaVO_4$:Eu^{3+} nanocrystals, Materials Chemistry and Physics 115 (2009) 165–171.
[21] C. Sungho, M.M. Young, J. Ha-Kyum, Luminescence properties of PEG-added nano crystalline YVO_4:Eu^{3+} phosphor prepared by hydrothermal method, J. Luminescence 130 (2010) 549–553.
[22] G. Liu, Y. Zhang, J. Yin, W.F. Zhang, Enhanced luminescence of Sm^{3+}/Bi^{3+} co-doped Gd_2O_3 phosphors by combustion synthesis, J. Luminescence 128 (2008) 2008–2012.
[23] Y. Porter-Chapman, C.E. Bourret, S.E. Derenzo, Bi^{3+} luminescence in $ABiO_2Cl$ (A=Sr, Ba) and $BABiO_2Br$, Journal of Luminescence 128 (2008) 87–91.
[24] F. Kellendonk, T. Vander Belt, G. Blasse, On the luminescence of bismuth, cerium, and chromium and yttrium aluminium borate, Journal of Chemical Physics 76 (3) (1982) 1194–1201.
[25] X.Y. Huang, X.H. Xu, Q.Y. Zhang, Broadband down conversion of ultraviolet light to near-infrared emission in Bi^{3+} - Yb^{3+} - co-doped Y_2O_3 phosphors, Journal of American Ceramic Society 94 (3) (2011) 833–837.
[26] A. Newport, J. Silver, A. Vecht, The synthesis of fine particle yttrium vanadate phosphors from spherical powder precursors using urea precipitation, Journal of Electrochemical Society 147 (2000) 3944–3947.
[27] S. Takeshita, T. Isobe, T. Sawayama, S. Niikura, Effects of the homogeneous Bi^{3+} doping process on photoluminescence properties of YVO_4:Bi^{3+}, Eu^{3+} nanophosphor, Journal of Luminescence 129 (2009) 1067–1072.
[28] G. Jamila, B. Herve, B. Michelle M.L. Jean, Spectroscopic study of $Bi_xEu_{1-x}VO_4$ and $Bi_yGd_{1-y}VO_4$ mixed oxides, Journal of Physics and Chemistry of Solids 50 (12) (1989) 1237–1244.
[29] X.Y. Huang, J.X. Wang, D.C. Yu, S. Ye, Q.Y. Zhang, X.W. Sun, Spectral conversion for solar cell efficiency enhancement using YVO_4:Bi^{3+}, Ln^{3+} (Ln=Dy, Er, Ho, Eu, Sm and Yb) phosphors, Journal of Applied Physics 109 (2011) 113526-1–113526-7.
[30] X. Wei, S. Huang, Y. Chen, C. Guo, M. Yin, W. Xu, Energy transfer mechanisms in Yb^{3+} doped YVO_4 near-infrared down conversion phosphor, Journal of Applied Physics 107 (2010) 103107-1–103107-5.
[31] G. Li, Z. Wang, M. Yu, Z. Quan, J. Lin, Fabrication and optical properties of core-shell structured spherical SiO_2@$GdVO_4$:Eu^{3+} phosphors via sol–gel process, Journal of Solid State Chemistry 179 (2006) 2698–2706.
[32] A.M. Pires, M.R. Davolos, E.B. Stucchi, Eu^{3+} as a spectroscopic probe in phosphors based on spherical fine particle gadolinium compounds, International journal of Inorganic Materials 3 (2001) 785–790.
[33] K. Vinay, K. Ravi, S.P. Lochab, S. Nafa, Effect of swift heavy ion irradiation on nano crystalline CaS: Bi phosphors: Structural, optical and luminescence studies, Nuclear Instruments and Methods in Physics Research B 262 (2007) 194–200.